Supplementary Information

Isolating metallophthalocyanine sites into graphene-supported microporous polyaniline enables highly efficient sensing of ammonia

Xiaodong Lu,[a] Zhimin Chen,*[a] Hao Wu,[a] Erping Cao,[a] Ying Wang,[a] Shichao Du,[a] Yiqun Wu*[ab] and Zhiyu Ren[a]

[a]Key Laboratory of Functional Inorganic Material Chemistry (Ministry of Education of China), School of Chemistry and Materials Science, Heilongjiang University, 74# Xuefu Road, Nangang District, Harbin 150080, People's Republic of China

[b]Shanghai Institutes of Optics and Fine Mechanics, Chinese Academy of Sciences, 390# Qinghe Road, Jiading District, Shanghai 201800, People's Republic of China

*Corresponding author E-mail: zmchen@hlju.edu.cn; yqwu@siom.ac.cn

Tel.: (+86) 451 8660 4331

Fax.: (+86) 451 8660 8616

Table of contents

1. Experimental Section

1.1. Synthetical of tetra-*β*-sulfophthalocyanine cobalt

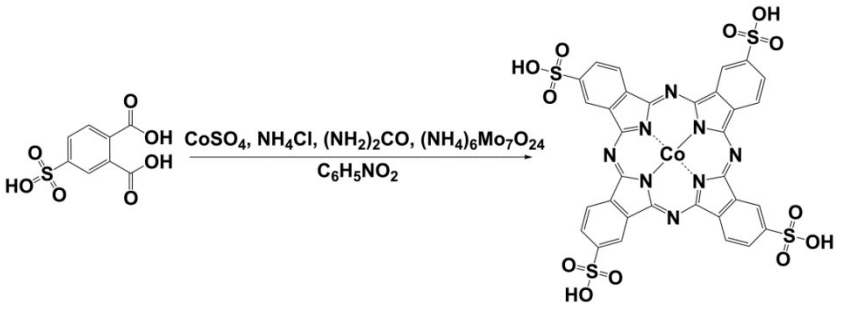

Scheme S1 Synthetical scheme of tetra-*β*-sulfophthalocyanine cobalt(II).

The synthetic scheme of tetra-*β*-sulfophthalocyanine cobalt(II) (CoTsPc) is shown in ***Scheme S1***.[S1,S2] Briefly, 4-sulfophthalic acid (4.32 g, 16.2 mmol), ammonium chloride (0.47 g, 9.0 mmol), urea (5.8 g, 97 mmol), ammonium molybdate tetrahydrate (0.068 g, 0.06 mmol), and anhydrous cobalt(II) sulfate (1.36 g, 4.8 mmol) were taken into a solution of freshly distilled nitrobenzene (100 mL) at room temperature. Then, the mixture was stirred for 6 h in oil bath at 180 ºC. After natural cooling to about 25 ºC, the precipitate was filtered, washed with methanol and hydrochloric acid (1 mol L^{-1}) saturated with sodium chloride, and then dissolved in a solution of sodium hydroxide (0.1 mol L^{-1}, 200 mL). Subsequently, the above solution was heated to 80 ºC and insoluble impurities were immediately separated by filtration. Then, the filtrate was acidified by addition of hydrochloric acid (0.1 mol L^{-1}, 200 mL) with stirring, and left to stand overnight. Finally, the resulting precipitate was collected by centrifugation, washed with 80 % aqueous ethanol and then dried in a vacuum oven at 80 ºC to obtained blue-black crystals of CoTsPc. Yield: 81 %. UV-vis spectra in DMF: λmax (nm) = 665, 618. FTIR spectra (KBr pellets) v: 3390, 1637, 1618, 1456, 1396, 1193, 1143, 1108, 1028, 931 and 634 cm^{-1}.

1.2. Calibration of gas concentration

The concentration of tested NH_3 gas is obtained by static volumetric capacity method. A series of commercially available standard gases with different concentrations and high purity ammonia act as the original gases, and the gases with target concentrations is obtained by diluting the desired volume of standards gas with air. The concentrations of tested gas were calculated using Eq. (1):

$$C_1V_1=C_2V_2 \quad (1)$$

where C_1 is the concentration of standard gas (ppm), V_1 is the volume of standard gas injected into the test chamber (mL), C_2 is the concentration of tested gas (ppm), and V_2 is the volume of test chamber (mL). Concentrations of standard gases and tested NH_3 were periodically calibrated by indophenol blue spectrophotometric method.

1.3. Detection limit calculation

Theoretical detection limits of devices were calculated by established procedure.[S3,S4] Briefly, the sensor noise was calculated using the variation in the relative sensor response in the baseline using the root-mean-square (RMS) deviation. We replotted 600 data points at the baseline before the NH_3 exposure. The points were averaged and a standard deviation (S). We then used Eq. (2) to calculate the RMS_{noise} of the sensors.

$$RMS_{noise} = \sqrt{\frac{S^2}{N}} \quad (2)$$

where N is the number of data points. According to the IUPAC definition,[S5] where the signal-to-noise ratio is 3. According to Figure 3C, the slope of the linear regression fit on the sensor response ($\Delta R/R_0$) vs gas concentration plot. We then used Eq. (3) to calculate the detection limit of the sensors.

$$Detection\ limit_{ppm} = 3\frac{RMS_{noise}}{slope} \quad (3)$$

Therefore, the theoretical NH_3 detection limit of the obtained RGO@PANI-CoTsPc-2 sensor was estimated to be 14 ppb.

1.4. Resistance of sensor device.

The resistance of the sensors device was measured with a CUST·G2 gas sensing test system (Advanced Sensor Technology Laboratory of Jilin University, China) recording the change in resistance passing through the sensor at a 1-s interval by a computer.

References:

S1. J. K. Joseph, S. L. Jain and B. Sain, *Ind. Eng. Chem. Res.*, 2010, **49**, 6674−6677.

S2. D. W. Scott, D. L. Myers, H. Hill and O. Omadoko, *Fuel*, 2019, **242**, 573−579.

S3. K. A. Mirica, J. G. Weis, J. M. Schnorr, B. Esser and T. M. Swager, *Angew. Chem. Int. Edit.*, 2012, **51**, 10740-

10745.

S4. V. Dua, S. P. Surwade, S. Ammu, S. R. Agnihotra, S. Jain, K. E. Roberts, S. Park, R. S. Ruoff and S. K. Manohar, *Angew. Chem. Int. Edit.*, 2010, **49**, 2154-2157.

S5. J. Li, Y. J. Lu, Q. Ye, M. Cinke, J. Han and M. Meyyappan, *Nano Lett.*, 2003, **3**, 929-933.

2. Supplementary Figures

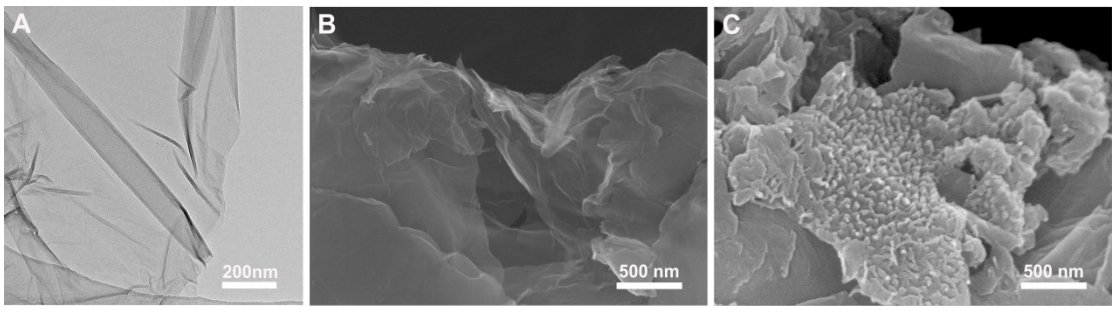

Fig. S1 TEM and SEM images of GO (A-B), SEM images of GO/CoTsPc (C).

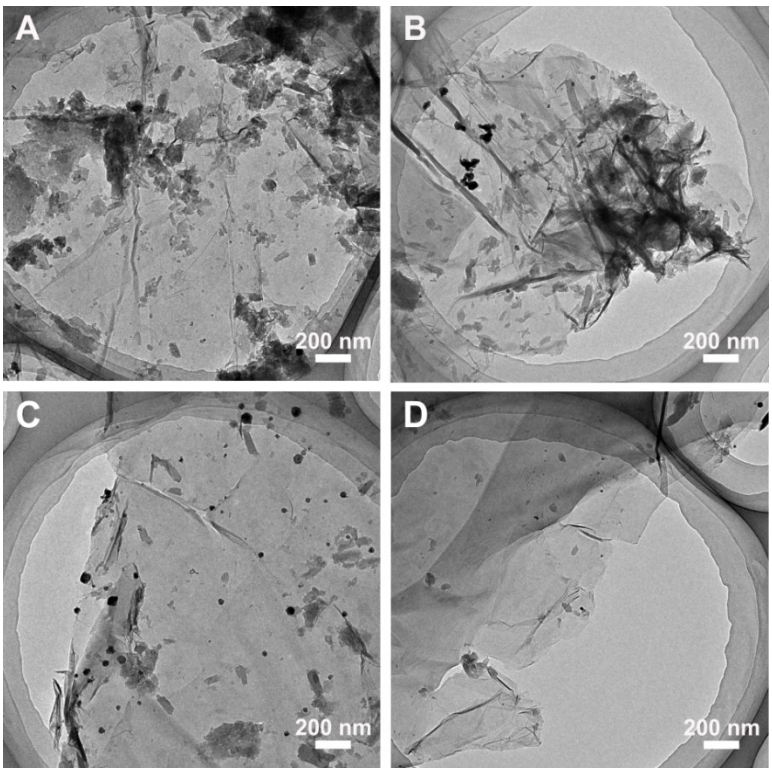

Fig. S2 TEM images of GO/CoTsPc/An samples prepared by changing the amount of An. The amount of An in (A−D) is 0, 27, 54 and 81 μL.

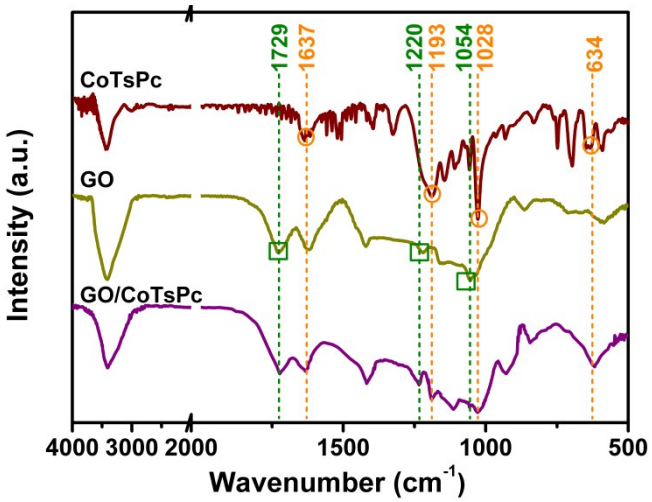

Fig. S3 FTIR spectra of CoTsPc, GO and GO/CoTsPc.

As shown in ***Fig. S3***, besides the typical vibrations of CoTsPc (1637, 1193, 1028 and 634 cm^{-1} assigned to C–C, S-O of SO_3^-, S=O and S-C), the typical bands of carbonyl and carboxyl groups (1729, 1220 and 1054 cm^{-1} assigned to C=O, C-OH, C-O) of GO are observed in the FTIR spectrum of the GO/CoTsPc hybrid, demonstrating the successful preparation of GO/CoTsPc. It is noteworthy that the slight shift in these peaks is due to electron delocalization of π-π interactions between GO and CoTsPc.

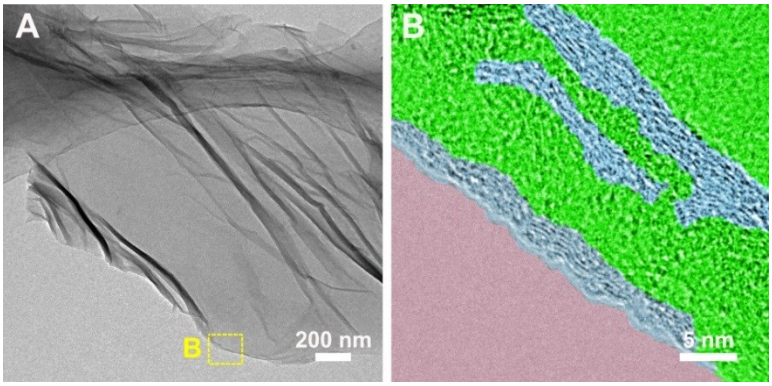

Fig. S4 TEM (A) and HRTEM (B) images of RGO@PANI-CoTsPc-2.

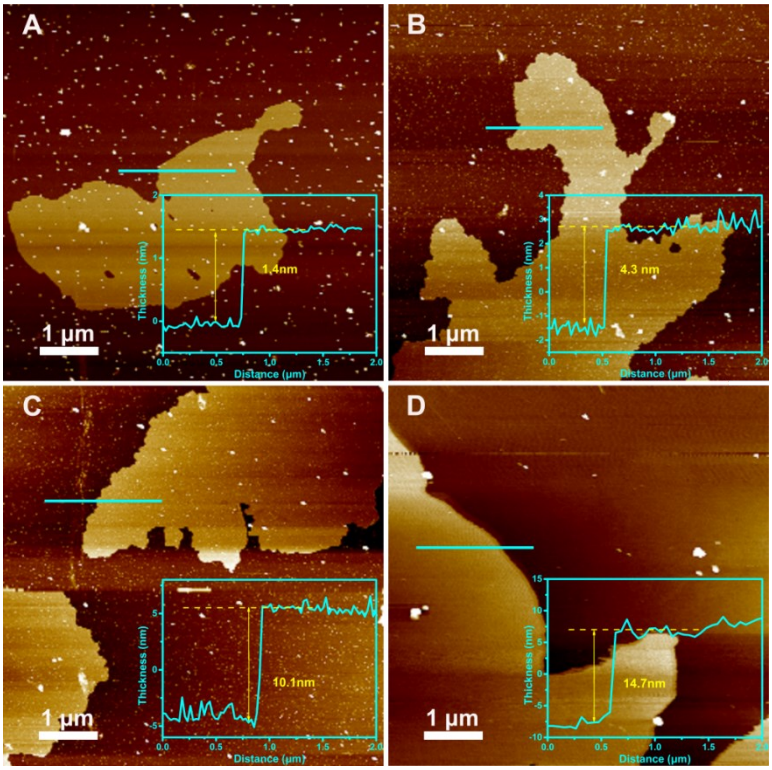

Fig. S5 Tapping-mode AFM topographic images and height profiles of GO (A), RGO@PANI-CoTsPc-1 (B), RGO@PANI-CoTsPc-2 (C) and RGO@PANI-CoTsPc-3 (D).

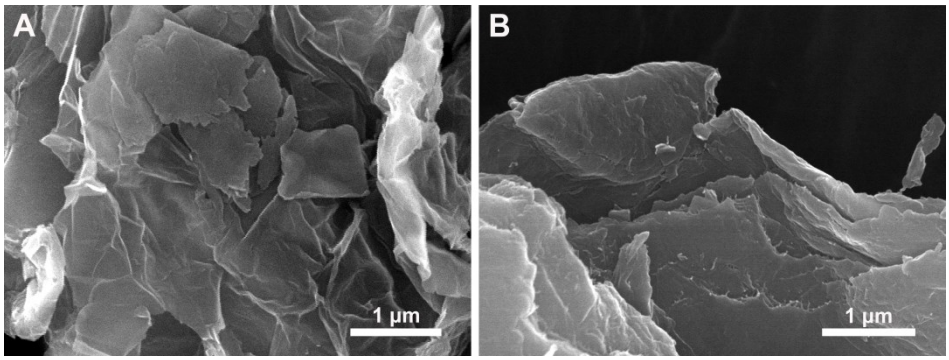

Fig. S6 SEM images of RGO@PANI-CoTsPc-1 (A) and RGO@PANI-CoTsPc-3 (B).

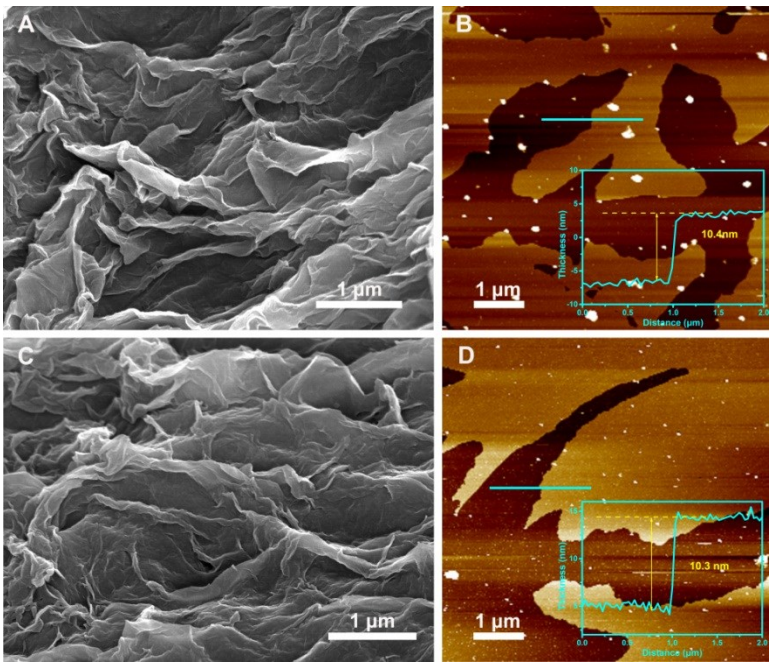

Fig. S7 SEM images, tapping-mode AFM topographic images and height profiles of RGO@PANI-0.5CoTsPc (A-B) and RGO@PANI-1.5CoTsPc (C-D).

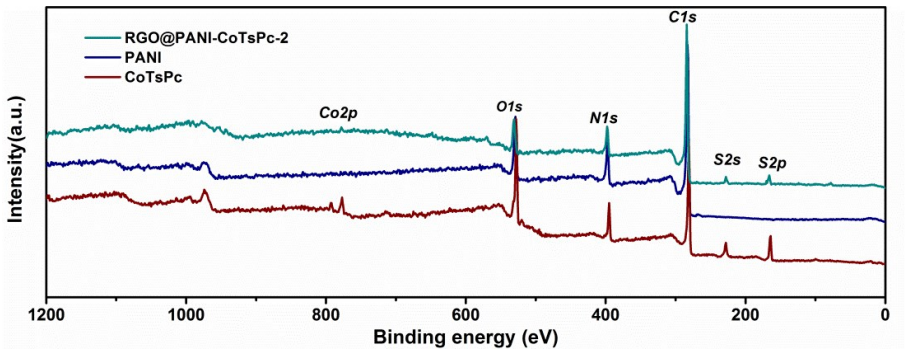

Fig. S8 XPS spectra of CoTsPc, PANI, and RGO@PANI-CoTsPc-2.

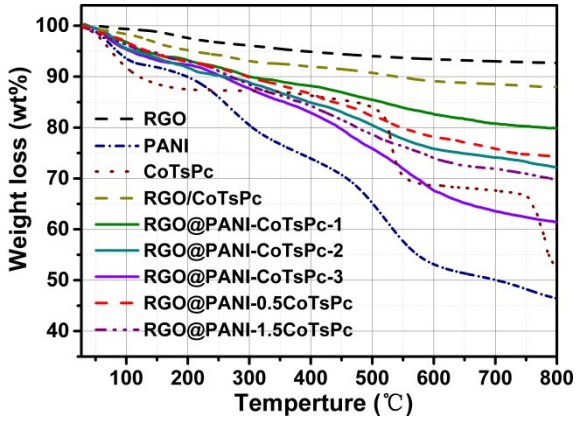

Fig. S9 TGA curves of RGO, PANI, CoTsPc, RGO/CoTsPc, RGO@PANI-CoTsPc-1, RGO@PANI-CoTsPc-2, RGO@PANI-CoTsPc-3, RGO@PANI-0.5CoTsPc and RGO@PANI-1.5CoTsPc measured under a N_2 atmosphere.

The weigh percent of CoTsPc assembled on RGO has been evaluated by TG analysis under N_2 atmosphere. As shown in ***Fig. S9***, TGA curve of CoTsPc presents a great loss of weight about 18.53 % from 300 to 600 ºC sharply, indicating the thermal decomposition of peripheral $–SO_3H$ groups in N_2 atmosphere. However, at the same temperature range, the weight loss of RGO/CoTsPc is about 3.97 %; and only a minor weight loss averaging 2.68 % for RGO. Taking into account the weight loss of RGO, a corrected weight loss of 1.29 % can be estimated, which comes from CoTsPc in RGO/CoTsPc. However, the actual amount of CoTsPc adsorbed on the surface of RGO should consider the weight loss of CoTsPc itself. So, a real ratio of 6.96 % (1.29/18.53 %) can be calculated. Using the same calculation method, the weigh percent of PANI in RGO@PANI-CoTsPc hybrids are also evaluated by TG analysis under N_2 atmosphere (***Fig. S9***), and the results are shown in ***Table S3***.

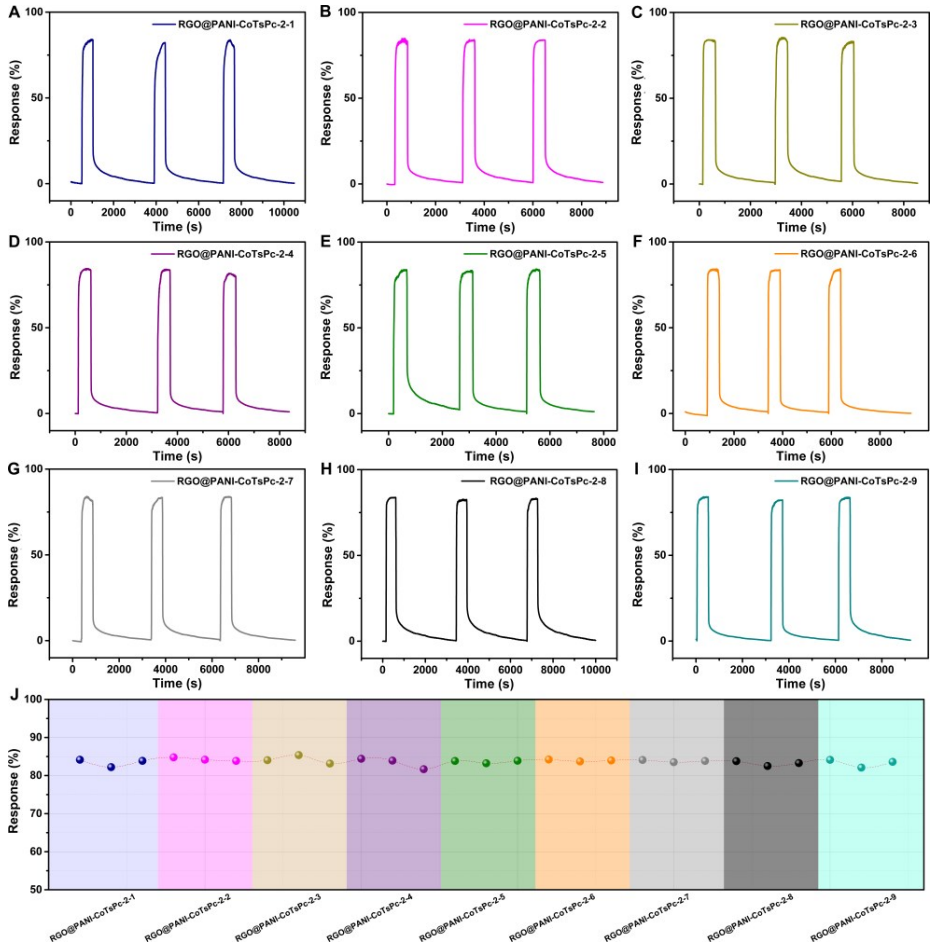

Fig. S10 Dynamic response curve (A-I) and response value (J) of RGO@PANI-CoTsPc-2-1, RGO@PANI-CoTsPc-2-2, RGO@PANI-CoTsPc-2-3, RGO@PANI-CoTsPc-2-4, RGO@PANI-CoTsPc-2-5, RGO@PANI-CoTsPc-2-6, RGO@PANI-CoTsPc-2-7, RGO@PANI-CoTsPc-2-8 and RGO@PANI-CoTsPc-2-9 upon exposure to 5 ppm NH_3.

As shown in ***Fig. S10***, RGO@PANI-CoTsPc-2 was prepared nine times using the same procedure by different experimental personnel and the obtained products were labeled as RGO@PANI-CoTsPc-2-1, RGO@PANI-CoTsPc-2-2, RGO@PANI-CoTsPc-2-3, RGO@PANI-CoTsPc-2-4, RGO@PANI-CoTsPc-2-5, RGO@PANI-CoTsPc-2-6, RGO@PANI-CoTsPc-2-7, RGO@PANI-CoTsPc-2-8 and RGO@PANI-CoTsPc-2-9, respectively. Compared with RGO@PANI-CoTsPc-2, all samples exhibited similar dynamic response curve and response value to 5 ppm of NH_3. This means that these products are basically the same, and the experiment can be easily reproduced by other researchers.

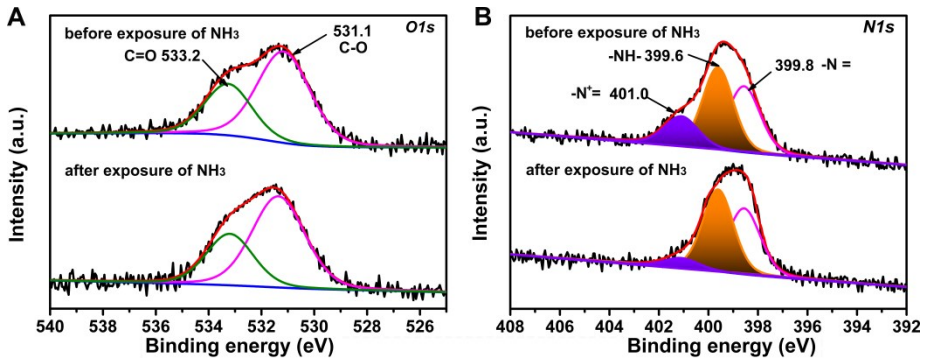

Fig. S11 High-resolution O 1s (A) and N 1s (B) XPS spectra of RGO@PANI sensor (top) before (top) and after (bottom) the exposure of NH_3.

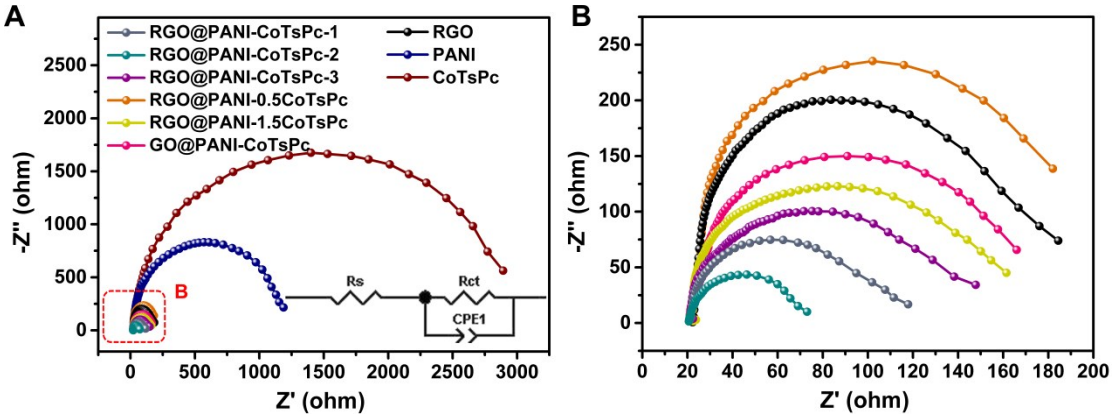

Fig. S12 Nyquist plots (A-B) of various RGO@PANI-CoTsPc, GO@PANI-CoTsPc, RGO, PANI and CoTsPc, the inset in *Fig. S12A* is the equivalent circuit model applied to fit the Nyquist plots, where R_s is the electrolyte resistance, R_{ct} is the charge-transfer resistance and CPE1 represent the double layer capacitance.

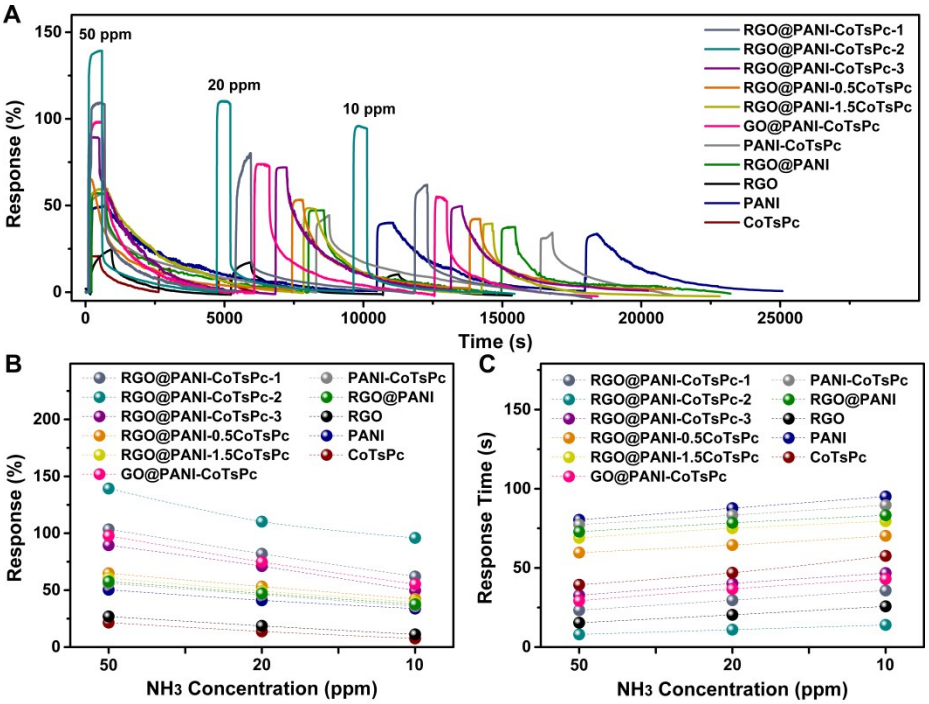

Fig. S13 The dynamic responses (A), response (B) and response time (C) of various RGO@PANI-CoTsPc, GO@PANI-CoTsPc, PANI-CoTsPc, RGO@PANI, RGO, PANI and CoTsPc toward 50, 20 and 10 ppm of NH_3 at room temperature.

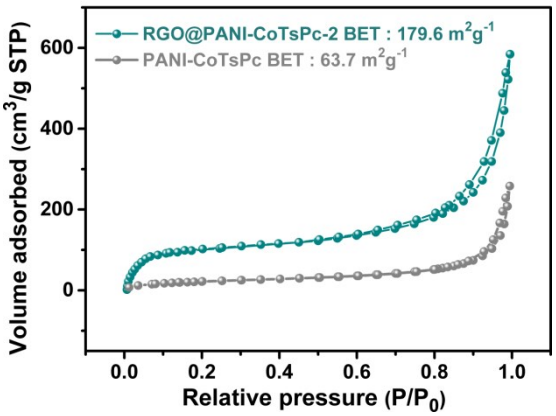

Fig. S14 N_2 adsorption-desorption isotherms of RGO@PANI-CoTsPc-2 and PANI-CoTsPc.

3. Supplementary Tables

Table S1 The detailed dosages of GO, CoTsPc, An, APS and hydrazine hydrate in the process of synthesizing control sample.

Sample name	GO (mg)	CoTsPc (mg)	An (μL)	APS (g)	hydrazine hydrate (mL)
RGO	50	0	0	0	2
PANI	0	0	54	0.135	0
GO/CoTsPc	50	4	0	0	0
RGO/CoTsPc	50	4	0	0	2
RGO@PANI	50	0	54	0.135	2
PANI-CoTsPc	0	4	54	0.135	0
GO/CoTsPc/An	50	4	54	0	0
GO@PANI-CoTsPc	50	4	54	0.135	0
RGO@PANI-0.5CoTsPc	50	2	54	0.135	2
RGO@PANI-1.5CoTsPc	50	6	54	0.135	2

Table S2 The content of CoTsPc in RGO@PANI-CoTsPc obtained from ICP-OES analysis.

Sensor material	CoTsPc content (wt%)
RGO@PANI-CoTsPc-1	7.15
RGO@PANI-CoTsPc-2	7.28
RGO@PANI-CoTsPc-3	7.37
RGO@PANI-0.5CoTsPc	3.79
RGO@PANI-1.5CoTsPc	10.56

Table S3 The amount of PANI in sensing materials obtained from TGA.

Sensing material	Weight loss from 300 to 600 °C (wt%)	PANI content (wt%)
RGO	2.68	0
CoTsPc	18.53	0
PANI	27.37	100.00
RGO/CoTsPc	3.97	0
RGO@PANI-CoTsPc-1	7.41	12.57
RGO@PANI-CoTsPc-2	13.15	33.54
RGO@PANI-CoTsPc-3	20.04	58.71
RGO@PANI-0.5CoTsPc	11.68	30.40
RGO@PANI-1.5CoTsPc	14.43	35.92

Table S4 The relationship of the response of RGO@PANI-CoTsPc-2 sensor to varying concentration of NH_3.

Sensing material	The concentrations ranging of NH_3 is from 0.05 to 2 ppm	The concentrations ranging of NH_3 is from 5 to 200 ppm	Detection limit (S/N = 3)
RGO@PANI-CoTsPc-2	$y = 20.315x + 9.292$ $R^2 = 0.999$	$y = 1.121x + 83.135$ $R^2 = 0.998$	14 ppb

Table S5 Room-temperature NH_3-sensing properties of different sensors.

Sensing material	Response (%) /Detection conc. (ppm)[b]	Detection limit (ppm)[a]	Response time (s) /Detectionv conc. (ppm)[b]	Recovery time (s) /Detection conc. (ppm)[b]	Reference
RGO@PANI-CoTsPc-2	***139.3/50***	***0.014***	***8/50***	***325/50***	***This work***
CuPc@IRMOF	~45/5	0.052	---	~1000/5	*Adv. Funct. Mater. 2020, 2005727.*
V-RGOH	10.1/20	0.42	149/20	284/20	*ACS Appl. Mater. Inter. 2020, 12, 20623.*
PPy/GO	42/10	---	110/10	650/10	*Adv. Funct. Mater. 2020, 30, 1909756.*
$Ti_3C_2T_x$ MXene/graphene	6.77/50	---	~600/50	~780/50	*ACS Appl. Mater. Inter. 2020, 12, 10434.*
PPy@rGO heterostructures	31/5	0.041	85/5	600/5	*ACS Appl. Mater. Interfaces 2020, 12, 38674.*
$LuPc_2$/Co(Cl_8Pc)	13/10	0.25	---	---	*ACS Sens. 2020, 5, 1849.*
PANI@SnO_2/Zn_2SnO_4	20.4/100	0.5	46/100	54/100	*Sensor. Actuat. B-Chem. 2020,317, 128218.*
$CsPbBr_3$	~0.1/50	8.85	10/50	30/50	*Small 2020, 16, 1904462.*
TiO_2–SnO_2/MWCNTs	~0.91/50	0.77	80/50	15/80	*J. Mater. Chem. C, 2020, 8, 7567.*
PCVA Hydrogel	31.6/40	~0.14	46/40	29/40	*ACS Sens. 2020, 5, 772.*
ZnO/Au	3.59/1	<0.01	---	---	*J. Hazard. Mater. 2020, 381, 120919.*
PPy/rGO	6.1/1	<1	60/1	300/1	*Sensor. Actuat. B-Chem. 2020,305, 127423.*
PANI/polysiloxane	~2.5/50	5	208/50	263/50	*Composites Part B 2020, 196, 108131.*

C/rGO wrapped Co_3O_4	123/50	---	20/50	300/50	*J. Mater. Chem. A, 2019, 7, 27522.*
RGO/TiO_2/Au	18.7/10	---	~100/10	---	*Anal. Chem. 2019, 91, 3311.*
Au-$MoSe_2$	2.6/20	---	18/20	16/20	*Nano Energy 2019,65, 103974.*
DPA-Ph-DBPzDCN	72.73/100	2	48/100	15/100	*J. Mater. Chem. A, 2019, 7, 4744.*
GCs/PANI	1.3/10	---	34/10	42/10	*ACS Sens. 2019, 4, 2343.*
$CuSbS_2$ /rGO	1.42/250	0.5	50/250	115/250	*ACS Appl. Mater. Interfaces 2019, 11, 9573.*
Ti_3C_2	6.13/500	---	45/25	94/25	*ACS Sens. 2019, 4, 2763.*
NiPc-M MOFs	43/80	0.16	~1800/80	---	*J. Am. Chem. Soc. 2019, 141, 2046.*
PANI/SWCNT	143/100	---	100/100	200/100	*ACS Appl. Mater. Interfaces 2019, 11, 38169.*
Q2D PANI	~2.1/10	0.03	~672/10	900/10	*Nat. Commun. 2019, 10, 4225.*
PANI/ WO_3	~7.5/100	0.5	13/10	49/10	*Sensor. Actuat. B-Chem. 2018, 259, 505.*
SiO_2CuMOF-GO-PANI	~59.3/40	0.6	30/40	180/40	*Anal. Chim. Acta 2018, 1043, 89-97.*
GO-PANI	31.8/100	0.05	102/10	186/10	*Sensor. Actuat. B-Chem. 2018, 273, 726.*
CFGO	121/500	0.006	86/500	116/500	*J. Mater. Chem. A, 2017, 5, 19116.*
Sulfonated RGO hydrogel	7.1/20	1.48	16/20	600/20	*Adv. Sci. 2017, 4, 1600319.*
PANI/MoS_2	~25/10	0.05	~170/10	---	*Small 2017, 13, 1701697.*
MCNT@1.0PANI	92.15/50	0.036	5/50	12/50	*J. Mater. Chem. A. 2017, 5, 24493.*

SiO_2@TRGO	6.5/50	---	250/50	---	*Nanoscale 2017, 9, 109.*
PANI/NiTsPc	275/100	---	10/100	46/100	*Sensor. Actuat. B-Chem. 2016, 226, 553.*
BPB/R-GO	5.5/25	5	210/25	~3600/25	*Adv. Funct. Mater. 2016, 26, 4329.*
Flexible PANI	19.48/100	---	33/100	131/100	*J. Mater. Chem. C 2015, 3, 9461.*
MWCNT/PANI	15.5/2	2	6/2	35/2	*Sensor. Actuat. B-Chem. 2015, 221, 1523.*
R-GO on 3D pillars	88/40	~1.5	720/40	~4800/40	*Adv.Funct. Mater., 2015, 25, 883-890.*
Cu_2O/rGO	104/200	---	28/200	204/200	*J. Mater. Chem. A, 2015, 3, 1174.*
HCSA doped PANI	~46/700	---	~600/700	~600/700	*Adv. Funct. Mater. 2014, 24, 4005.*
PANI@CNT	7.3/2500	50	1200/2500	---	*J. Mater. Chem. A 2013, 1, 13321.*
RGO	23/2800	---	~600/2800	~1200/2800	*ACS Appl. Mater. Interfaces 2013, 5, 7599.*
PANI/RGO	59.2/50	---	~1080/50	---	*J. Mater. Chem. 2012, 22, 22488.*

[a] If the sensor detection limit was not explicitly provided in the original report, then the lowest tested analyte concentration is listed.

[b] If the response (%), response time (s) or recovery time (s) of the sensor was not explicitly provided in the original report, then the estimate from the curve in that report is listed.

Abbreviations: RGO = Reduce graphene oxide; PANI= Polyaniline; Pc = phthalocyanine; IRMOF= isoreticular MOF; V-RGOH = vitamin C (VC)-modified reduced graphene hydrogel; PPy = Polypyrrole; GO = Graphene oxide; LuPc = lutetium phthalocyanine; PCVA = Polymer chains of poly(vinyl alcohol) (PVA) and carrageenan (CA); C = amorphous carbon; GCs = graphite capsules; DPA-Ph-DBPzDCN = 3,6-bis(4-(diphenylamino)phenyl)dibenzo[a,c]phenazine-11,12-dinitrile; M = Ni, Cu; SWCNT = single-walled carbon nanotube; Q2Ds = quasi-two-dimensional; MOF = metal-organic frameworks; CFGO = chemically fluorinated graphene oxide; MWCNT = Multi-walled carbon nanotube; BPB = bromophenol blue; HCSA = (+)-cam-phor-10-sulfonic acid; CNT = Carbon nanotube; SWNT = Single walled carbon nanotube.

Table S6 Parameters obtained by fitting the Nyquist plots of various RGO@PANI-CoTsPc, GO@PANI-CoTsPc, RGO, PANI and CoTsPc using the equivalent circuit in *Fig. S12A*.

Samples	R_s (Ω)	R_{ct} (Ω)	CPE1 (F)
RGO@PANI-CoTsPc-1	21.10	85.49	3.96×10^{-5}
RGO@PANI-CoTsPc-2	21.02	52.84	4.25×10^{-5}
RGO@PANI-CoTsPc-3	21.14	117.26	3.67×10^{-5}
RGO@PANI-0.5CoTsPc	22.39	157.74	3.13×10^{-5}
RGO@PANI-1.5CoTsPc	21.28	127.73	3.54×10^{-5}
GO@PANI-CoTsPc	21.44	134.11	3.38×10^{-5}
RGO	21.83	144.98	3.29×10^{-5}
PANI	22.78	1132.26	0.46×10^{-5}
CoTsPc	22.95	2750.01	1.17×10^{-4}